IL NUOVO CIMENTO **44 C** (2021) 4
DOI 10.1393/ncc/i2021-21004-y

Communications: SIF Congress 2020

First direct measurement of the neutron Sachs magnetic form factor

G. Mezzadri([1])([2])([*])

([1]) *INFN, Sezione di Ferrara - Ferrara, Italy*
([2]) *Institute of High Energy Physics of Chinese Academy of Sciences - Beijing, China*

received 31 January 2021

Summary. — The BESIII experiment has collected data samples between 2 and 3.08 GeV to study baryons cross sections and form factors. While there are many measurements of the $e^+e^- \to p\bar{p}$ cross section, the knowledge of the $n\bar{n}$ final state is scarce. In this paper, the analysis of this final state by the BESIII Collaboration will be presented. This analysis uses three different strategies to maximize the neutron detection efficiency. This lead to the world's most precise measurement of the $e^+e^- \to n\bar{n}$ cross section and the first direct measurement of the magnetic form factor of the neutron.

1. – Introduction

Since the discovery of the not pointlike behaviour of protons and neutrons, the study on their charge and magnetic moment spatial distribution has been of the utmost interest. For decades the study has been focused to the deep inelastic scattering (DIS) approach, where a projectile (electrons, neutrinos) is used to investigate the structure of the baryon. This allowed a deep investigation of the so-called spacelike part of the spectrum.

In the last 30 years, owing to the ever-growing precision of the experimental spectrometers, it has been possible to study also the timelike region, by studying the annihilation process, mostly at e^+e^- colliders. This has brought to a great number of results for the proton form factor. Given the zero charge of the neutron, and thus a much more lower efficiency in the reconstruction of the final state, the information on the neutron form factor is widely less precise: the few measurements available in the literature [1-4] have poor precision. Moreover, a better knowledge will allow a comparison with the measurements performed in the spacelike region and with the proton behaviour.

([*]) On behalf of the BESIII Collaboration.

In this article, we present the most precise measurements of the neutron anti-neutron cross section and neutron effective form factor at the center of mass between 2 and 3.08 GeV made by the BESIII Collaboration. By combining some of the datasets to increase the statistics, the first direct measurement of the neutron magnetic form factor is reported. The article is structured as follows: first a brief introduction on the baryon form factor in the timelike region is presented, followed by the description of the BESIII experiment; later, the selection criteria to identify the neutrons are shown, and a full discussion of the results found is presented at last. All the results are to be considered preliminary.

1·1. *Baryon form factor*. – Form factors have been introduced to describe the composite nature of the baryons. In the annihilation process, as shown in fig. 1, the $\gamma B\bar{B}$ current can be written in terms of the Pauli Form Factors F_1 and F_2:

$$\Gamma^\mu = \gamma^\mu \mathrm{F}_1^N(q^2) + \frac{i\sigma^\mu_\nu q^\nu}{2M}\mathrm{F}_2^N(q^2),$$

where M is the baryon mass, q^μ is the transferred momentum. It is possible to define other two form factors, as a linear combination of the Pauli form factors. These are the so-called Sachs Form Factors and can be written as $G_E(q^2) = F_1(q^2) + (q^2/4M^2)F_2(q^2)$ and $G_M(q^2) = F_1(q^2) + F_2(q^2)$. These factors represent the Fourier transformation of the charge and the magnetic moment of the baryons and thus are called the electric and the magnetic form factor, respectively. The Born cross section of the process in fig. 1 can be written as

$$\sigma_{Born} = \frac{4\pi\alpha^2\beta C(q^2)}{3q^2}\left[|G_M(q^2)|^2 + |G_E((q^2)|^2\frac{1}{2\tau}\right], \tag{1}$$

where α is the electromagnetic (EM) fine structure constant, β is the final state particle velocity, $\tau = \frac{q^2}{m_B^2}$ and m_B is the mass of the baryon, and $C(q^2)$ is the Coulomb correction factor [5].

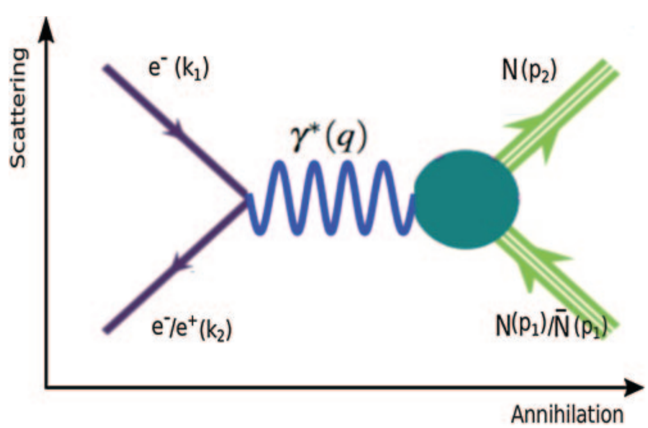

Fig. 1. – Sketch of the annihilation process at e^+e^- factories.

It is also possible to define an additional form factor, usually called *effective* form factor, that is proportional to the Born cross section σ_{Born}:

$$|G_{eff}| = \left(\frac{3q^2}{4\pi\alpha^2\beta\left(1+\frac{2m_B^2}{q^2}\right)} \right)^{\frac{1}{2}} \sqrt{\sigma_{Born}}, \tag{2}$$

where α is the EM fine structure constant, β is the baryon velocity, and m_B is the baryon mass.

To extract the magnetic form factor experimentally, it is necessary to study the angular differential cross section, that can be written as

$$\frac{\mathrm{d}\sigma^{Born}_{B\bar{B}}}{\mathrm{d}\cos\theta_{\bar{B}}} = A \times |G_M|^2 \left[\left(1+\cos^2\theta_{\bar{B}}\right) + R^2_{em}\frac{4M_n^2}{s}\left(1-\cos^2\theta_{\bar{B}}\right) \right], \tag{3}$$

where A is a normalization term, $\theta_{\bar{B}}$ is the angle of the outcoming antibaryon, and $R_{em} = |\frac{G_E}{G_M}|$ is the ratio between the electric and the magnetic form factor.

1˙2. *BESIII experiment and dataset.* – The BESIII (BEijing Spectrometer III) experiment is a multipurpose detector optimized for flavor physics. Its physics program is rich and covers charmonium(-like) and light hadrons spectroscopy, charmed mesons and baryons decays, τ lepton measurements, QCD studies and New Physics studies. To perform these studies, it collects data coming from the collision provided by the electron-positron collider BEPCII (Beijing Electron Positron Collider - II), that is able to shift its center-of-mass energy in the energy range between 2 and 4.9 GeV. The accelerator complex is hosted the Institute of High Energy Physics of Beijing, PRC.

The spectrometer covers 93% of 4π with a barrel and two endcaps. It is composed by: i) a Helium-based Multi-layer Drift Chamber (MDC), that, together the 1 tesla solenoidal magnetic field, allows for the measurement of the particles charge, position and momentum; ii) plastic scintillators to operate as Time-Of-Flight (TOF) detectors, that contribute to the particle identification together with the energy loss per unit length (dE/dx) in the MDC; iii) a CsI(Tl) Electro-Magnetic Calorimeter (EMC) to determine the particle energy and reconstruct the photon candidates; and iv) layers of Resistive Plate Counters (RPC) to operate as Muon Counters (MUC), placed in the return yoke of the magnet. More details on the detector can be found in ref. [6].

2. – The analysis

The used dataset consists of 16 energies from 2 to 3.08 GeV for a total integrated luminosity of 651 pb^{-1} and it has been collected in 2015 for precise R measurement. In order to maximize the neutron and anti-neutron detection efficiency, three different mutually exclusive event selections have been prepared, based on the interaction of the hadrons with TOF and EMC.

2˙1. *Neutron reconstruction strategy.* – The starting point is to search for events with zero charged tracks and a signal in the EMC compatible with the annihilation of the anti-neutron with one of the calorimeter nuclei.

The next selection applied is the request of a signal in the TOF detector: the annihilation can produce also particles that can produce a signal. If there is no signal, the event are stored as type "C": both the neutron and the anti-neutron signals are reconstructed only using the information of the EMC.

If there is a signal in TOF in correspondence to the signal in the EMC, a signal is searched in the TOF in the opposite side of the detector. If there is no signal, the events are stored as type "B": the anti-neutron is reconstructed with the information of the EMC+TOF, while the neutron signal is reconstructed only with the TOF. Instead, if there is a signal in the TOF, the events are stored as type "A": in these events, the anti-neutron is still reconstructed using both TOF and EMC signals, but the neutron is reconstructed by only the TOF information.

2·2. *Counting the neutrons.* – Since each type of events is reconstructed with different techniques, the number of events is extracted separately for each category and then a weighted mean is applied to find the final results.

To count the "A" events, the time of the neutron in the TOF is compared to the expected value by analytic calculation. This distribution shall peak around zero. The opening angle between the neutron and the anti-neutron is used to discriminate between signal and background in the type "B" and "C" events. Since it is a two-body decay, the opening angle shall peak at 180°. Figure 2 shows the three distributions for the dataset at 2.396 GeV, that is one with the largest luminosity.

A clear signal is visible in the expected regions for all three samples. In the left plot (type "A" events), a second peak is visible: these events come from the $e^+e^- \to \gamma\gamma$ process, an irremovable background source. The two are well separated, thus the analysis is not affected. The signal shape extracted from Montecarlo samples is used for the event type "A", while the signal in "B" and "C" types is described by a Crystal Ball function.

3. – Results and discussion

3·1. *Born cross section extraction.* – The Born cross section for each event category and center-of-mass energy can be extracted from the following formula:

$$\sigma_{Born} = \frac{N_{data}}{\varepsilon^M_{n\bar{n}} C \times \mathcal{C}_{dm} \times \mathcal{C}_{trg} \times (1+\delta) \times \mathcal{L}_{int}}, \tag{4}$$

where $\varepsilon^M_{n\bar{n}} C$ is the efficiency extracted from the Montecarlo simulations, $\mathcal{C}_{dm}$ is a term that takes in account the differences between data and MC, $\mathcal{C}_{trg}$ is the trigger efficiency,

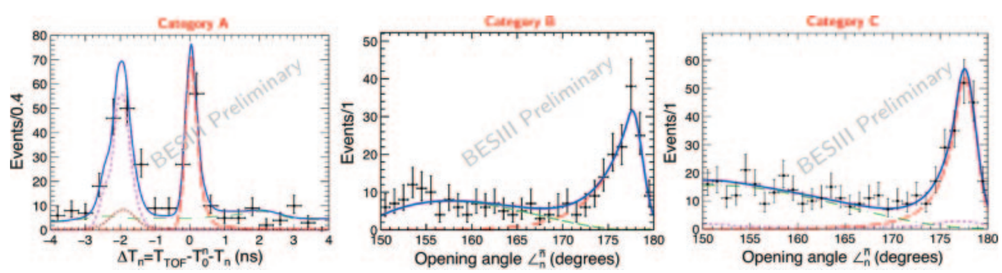

Fig. 2. – Results from the fit to the data at 2.396 GeV. Data are shown as points with error bars. Solid lines represent the total fit, dashed lines are the signal component, while dotted ones are from the background contributions.

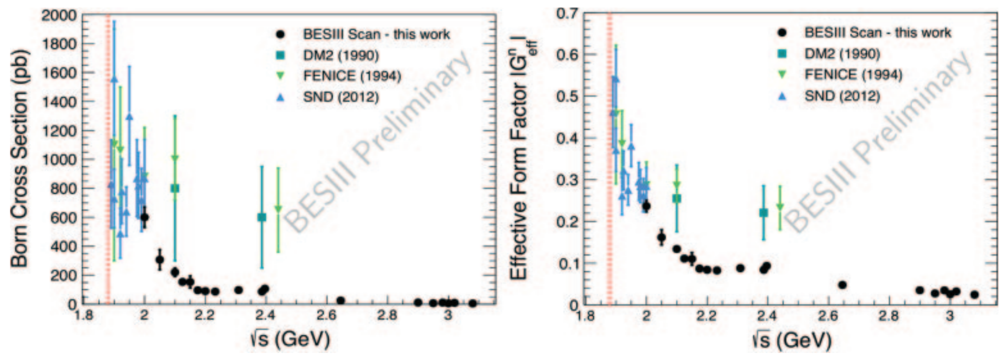

Fig. 3. – Comparison of the results of this work with other recent results. Black dots are the results of this work, squares represents the results from ref. [1], pointing down triangles are from ref. [2], and pointing up triangles are from refs. [3,4]. Left: Born cross section. Right: effective form factor.

$(1+\delta)$ is the radiative correction term, $\mathcal{L}_{int}$ is the luminosity of the sample, and N_{data} is the number of fitted events. The left plot of fig. 3 shows the results compared with the other available measurements.

The BESIII one is the most precise measurement so far, with a precision better than 10% at 2.396 GeV. The result at 2 GeV is compatible with the most recent measurement of SND [3, 4], while the other energies are systematically lower than all the previous measurements, even though they are in agreement due to the large errors of the previous measurements.

With the results of the Born cross section it is possible to extract the effective form factor from eq. (2). The right plot of fig. 3 shows the results compared with the previous measurements. Also in this case, the BESIII measurement is the most precise one and it is systematically lower than the previous results.

3˙2. *Comparison with the proton cross section.* – Proton and neutron are members of an isospin doublet and in the quark model they differ from each other by just the third valence quark. So it is straightforward to compare their behaviour. Figure 4 shows the ratio of the results found in this work with respect to recent BESIII publications on the process $e^+e^- \to p\bar{p}$ [7,8].

It is interesting to note that the ratio seems to change at 2.4 GeV. After this value, the ratio becomes closer to $R \sim 1$, that is the expected results predicted by perturbative QCD [9]. Before this value the ratio is flat and smaller, compatible with the squared ratio of the quark charge $R \sim |\frac{q_d}{q_u}| \sim 0.25$, as if in this energy regime the electromagnetic interaction is dominant with respect to the strong one. The point at 2 GeV is higher than the other points in this regime: further studies may be needed to understand whether this enhancement may be due an additional effect at threshold [10].

3˙3. *R_{em} and the Sachs magnetic form factor.* – As appears clear from eq. (3), in order to access to the $R_{em} = |\frac{G_E}{G_M}|$ it is necessary to fit the angular distribution of the anti-neutron. In order to achieve a more precise results, several datasets with lower luminosity are joined together to increase the statistics. Figures 5(a) and 5(b) show the fitted values for each energy interval. In this analysis, only five intervals are then extracted. The error on the X-axis of the plots indicates that the all

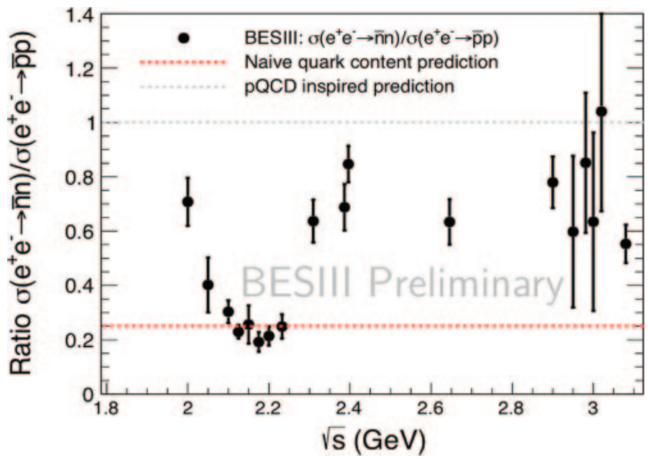

Fig. 4. – Ratio between the $\sigma(e^+e^- \to n\bar{n})$ and $\sigma(e^+e^- \to p\bar{p})$ cross sections using all recent BESIII data. Two theoretical predictions are also showed to magnifiy the different behaviour in the two energy regions.

datasets in that region are used. The data are also corrected for possible geometrical inefficiencies.

These are the first direct measurements of the magnetic form factor. The results are still dominated by the statistical error. Nevertheless, it is possible to extract some information. First, $|R_{em}| \sim 1$, that implies $G_E \neq 0$. This is completely unexpected, since all previous measurements always assumed the electric form factor equal to zero, as done for the FENICE data shown in fig. 6. It is possible to compare the obtained results with several models [11-14]. The best fit is provided by the Mainz model [13], that is a dispersion relation analysis based on all the most recent data available for proton and neutron in both timelike and spacelike regions.

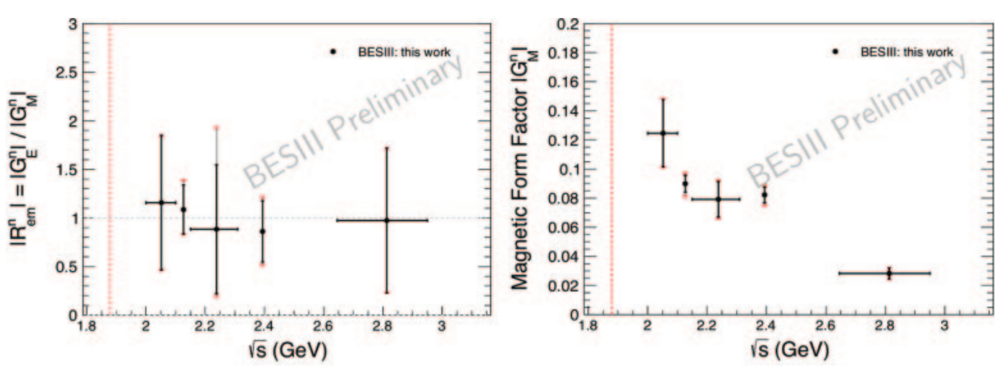

Fig. 5. – Results of the angular analysis to extract information of the neutron form factors. Vertical solid bars represents the statistical error, while the extended dashed bar with the arrow represents the systematic contribution. Horizontal bars represents the energy interval considered to extract the central value. (a) Ratio between the electric and the magnetic form factor. (b) First direct measurements of the magnetic form factors.

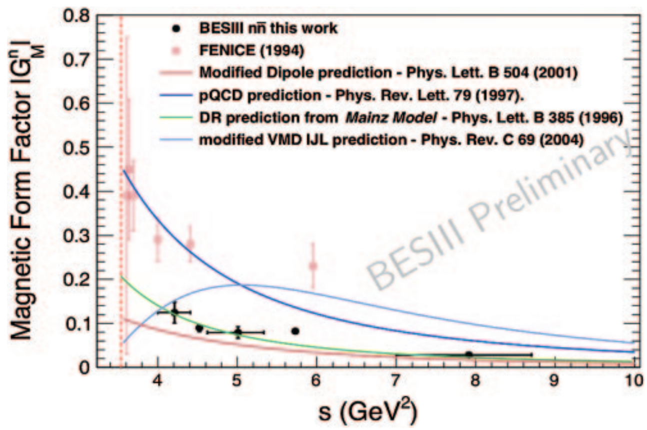

Fig. 6. – Comparison between the available measurements of the magnetic form factor and different theoretical models. Black dots are from this work, while squares are from ref. [2].

4. – Summary

The study of the form factors will help in providing important information on the structure of the hadrons. The BESIII Collaboration is playing a major role owing to the great performance of the detector and the accelerator complex, collecting data sample at different center of mass energies. This analysis profits of the great knowledge of our detector, enhancing the efficiency by extracting different categories of neutron events.

In this work, the most precise measurement of the $e^+e^- \to n\bar{n}$ cross section in the energy range between 2 and 3.08 GeV is presented. By extracting the ratio with recent measurements on the $e^+e^- \to p\bar{p}$, it is possible to identify two regions in which two different interactions seem to dominate.

Moreover, by fitting the angular distribution it has been possible to measure for the first time the neutron Sachs magnetic form factor and to extract that the electric one is different from zero. These results are still limited by statistics. However, BESIII has plans to collect 10 years more of data [15]: new datasets will be made available to further increase the knowledge on the electric and magnetic properties of the neutron in the timelike region.

* * *

The author is supported by the President Initiated Fellowship Initiative of the Chinese Academy of Sciences and by the STRONG-2020 project of the European Union's Horizon 2020 research and innovation programme under grant agreement No. 824093.

REFERENCES

[1] DM2 Collaboration (Bisello D. *et al.*), *Z. Phys. C*, **48** (1990) 23.
[2] FENICE Collaboration (Antonelli A. *et al.*), *Nucl. Phys. B*, **517** (1998) 3.
[3] SND Collaboration (Achasov M. N. *et al.*), *Phys. Rev. D*, **90** (2014) 112007.
[4] Druzhinin V. P. and Serednyakov S. I., *EPJ Web of Conferences*, **212** (2019) 07007.
[5] Arbuzov A. B. and Kopylova T. V., *JHEP*, **04** (2012) 009.
[6] BESIII Collaboration (Ablikim M. *et al.*), *Nucl. Instrum. Methods A*, **614** (2010) 345.

[7] BESIII Collaboration (Ablikim M. *et al.*), *Phys. Rev. Lett.*, **124** (2020) 042201.
[8] BESIII Collaboration (Ablikim M. *et al.*), *Phys. Rev. D*, **99** (2019) 092002.
[9] Pacetti S. *et al.*, *Phys. Rep.*, **550-551** (2015) 1.
[10] Baldini Ferroli R. *et al.*, *Eur. Phys. J A*, **48** (2012) 33.
[11] Karanikas A. I. and Stefanis N. G., *Phys. Lett. B*, **504** (2001) 291.
[12] Shirkov D. V. and Solovtsov I. L., *Phys. Rev. Lett.*, **79** (1997) 1209.
[13] Hammer H. W., Ulf-G. Meissner and Drechsel D., *Phys. Lett. B*, **385** (1996) 343.
[14] Bijker R. and Iachello F., *Phys. Rev. C*, **69** (2004) 068201.
[15] BESIII Collaboration (Ablikim M. *et al.*), *Chin. Phys. C*, **44** (2020) 040001.